Applied Surface Science 458 (2018) 700–704

Contents lists available at ScienceDirect

Applied Surface Science

journal homepage: www.elsevier.com/locate/apsusc

Full Length Article

Preparation and optical properties of higher manganese silicide, (Mn,Fe)Si_γ, thin films

Kei Hayashi*, Kentaro Ishii, Chihiro Kawasaki, Ryosuke Honda, Yuzuru Miyazaki

Department of Applied Physics, Graduate School of Engineering, Tohoku University, Sendai 980-8579, Japan

ARTICLE INFO

Keywords:
Higher manganese silicide
Fe substitution
Electronic structure
Pulsed laser deposition
Epitaxial growth
Optical absorption

ABSTRACT

In this article, the optical properties of thin films of higher manganese silicide (HMS) systems, $MnSi_\gamma$ and (Mn,Fe)Si_γ, were investigated. Band structure calculations were performed using the $Mn_{11}Si_{19}$ and $(Mn_{31/44}Fe_{13/44})_{11}Si_{19}$ crystal structure models of HMS to predict the conduction types and band gaps of $MnSi_\gamma$ and $Mn_{0.7}Fe_{0.3}Si_\gamma$, respectively. Using a pulsed laser deposition method, p-type $MnSi_\gamma$ and n-type $Mn_{0.7}Fe_{0.3}Si_\gamma$ thin films with *a*-axis orientation were grown on R-sapphire substrates. The measured direct band gaps were 0.81(1) eV for the $MnSi_\gamma$ thin film and 0.83(2) eV for the $Mn_{0.7}Fe_{0.3}Si_\gamma$ thin film. These results demonstrate the potential of (Mn,Fe)Si_γ-based near-infrared absorption solar cells.

1. Introduction

Higher manganese silicide (HMS) has attracted attention as a functional material for thermoelectric and optoelectronic devices [1–3]. There are several crystal structure models for HMS; Mn_4Si_7 [4], $Mn_{11}Si_{19}$ [5], $Mn_{15}Si_{26}$ [6], $Mn_{27}Si_{47}$ [7] and $MnSi_\gamma$ [8]. The last model is a (3 + 1)-dimensional crystal structure model which comprises the other four three-dimensional crystal structure models. The γ value in the chemical formula $MnSi_\gamma$ is the Si/Mn ratio in the Mn subsystem (i.e., the ratio of the *c*-axis length of the Mn subsystem to that of the Si subsystem). It is known that HMS is a p-type semiconductor. Using the three-dimensional crystal structure models, the band gap of HMS was calculated to be 0.769 eV (Mn_4Si_7) and 0.78 eV ($Mn_{11}Si_{19}$, $Mn_{15}Si_{26}$ and $Mn_{27}Si_{47}$) [9]. Thus, it is expected that HMS can be applied in near-infrared (NIR) absorption solar cells. However, there have been various reports on the band gap of HMS in the cases of bulk [10–12] and thin films [13–17]; indirect and direct band gaps ranging from 0.4 eV to 0.96 eV have been reported.

Recently, we successfully fabricated highly-oriented $MnSi_\gamma$ thin films on R-sapphire substrates using a pulsed laser deposition method [18]. The orientation relationship was found to be $MnSi_\gamma$ (1 0 0 0) [0 0 1 0]//Sapphire (1 $\bar{1}$ 0 2)[1 1 $\bar{2}$ 0]. (The $MnSi_\gamma$ (1 0 0 0) face corresponds to the (1 0 0) face of the Mn subsystem.) The conduction type of the $MnSi_\gamma$ thin film is p-type, which is confirmed by the fact that $MnSi_\gamma$ thin films possess positive Seebeck coefficients. In order to realise an NIR absorption solar cell based on HMSs, an n-type counterpart to the p-type $MnSi_\gamma$ thin film is desired. Since $(Mn_{0.7}Fe_{0.3})Si_\gamma$ bulk is known to exhibit n-type conduction due to the increase in electron carriers by the Fe substitution in some experimental studies [19–22], we fabricated an $(Mn_{0.7}Fe_{0.3})Si_\gamma$ thin film to act as the n-type counterpart. In addition, the band gaps of the $MnSi_\gamma$ and $(Mn_{0.7}Fe_{0.3})Si_\gamma$ thin films were evaluated.

2. Calculation and experimental methods

The electronic band structures of $MnSi_\gamma$ and $(Mn_{0.7}Fe_{0.3})Si_\gamma$ were calculated using the crystal structure models of $Mn_{11}Si_{19}$ and $(Mn_{31/44}Fe_{13/44})_{11}Si_{19}$ (i.e., $(Mn_{\sim 0.70}Fe_{\sim 0.30})_{11}Si_{19}$) as shown in Fig. 1(a) and (b), respectively. These models have an Si/Mn ratio (1. $\dot{7}\dot{2}$) between the γ values of $MnSi_\gamma$ (γ ~ 1.7361(1) [8]) and $Mn_{0.7}Fe_{0.3}Si_\gamma$ (γ ~ 1.6814(3) [22]). The lattice parameters of $Mn_{11}Si_{19}$ were the same as those used in a previous calculation (*a* = 5.500 Å and *c* = 44.881 Å [9]). The lattice parameters of $(Mn_{31/44}Fe_{13/44})_{11}Si_{19}$ were set at *a* = 5.451 Å and *c* = 44.522 Å, because it has been reported that a 30% Fe substitution in $MnSi_\gamma$ leads to a 0.9% and a 0.8% decrease in the *a*- and *c*-axis lengths of the Mn subsystem, respectively [22]. The Mn/Fe and Si atomic positions in $Mn_{11}Si_{19}$ and $(Mn_{31/44}Fe_{13/44})_{11}Si_{19}$ were identical with those reported in [5]. The band calculation was based on the density functional theory with the Perdew-Burke-Ernzerh parameterised generalised-gradient-approximation using the WIEN2k code [23]. The total number of *k*-points in the irreducible Brillouin zone was ten for $Mn_{11}Si_{19}$ and eight for $(Mn_{31/44}Fe_{13/44})_{11}Si_{19}$. The separation energy between valence and core states was -7.0 Ry, and the cut-off energy was 200 eV.

* Corresponding author.
E-mail address: hayashik@crystal.apph.tohoku.ac.jp (K. Hayashi).

https://doi.org/10.1016/j.apsusc.2018.07.141
Received 19 April 2018; Received in revised form 6 July 2018; Accepted 20 July 2018
Available online 21 July 2018
0169-4332/ © 2018 Elsevier B.V. All rights reserved.

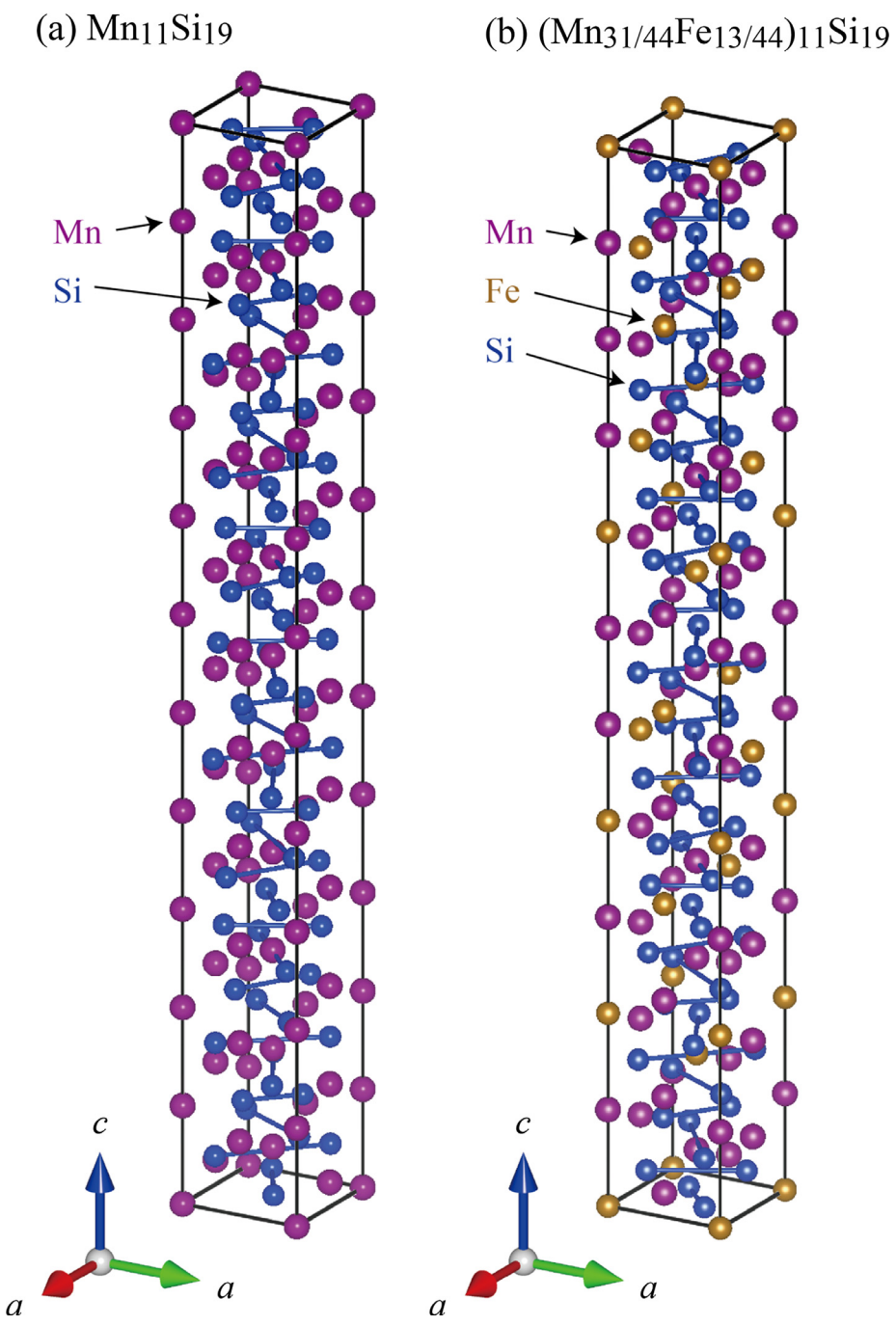

Fig. 1. Crystal structure models used for the electronic band structure calculations: (a) $Mn_{11}Si_{19}$ and (b) $(Mn_{31/44}Fe_{13/44})_{11}Si_{19}$.

Mn (purity: 3 N), Fe (purity: 3 N) and Si (purity: 4 N) powders were weighed and mixed according to the nominal compositions of $MnSi_2$ and $Mn_{0.7}Fe_{0.3}Si_2$. For each system, the mixed powder was arc-melted to prepare an ingot. The ingot was pulverised and then sintered by spark plasma sintering at 1123 K for 3 min under an applied pressure of 50 MPa (SPS, 520S, Fuji Electric Industrial Co. Ltd.) to obtain $MnSi_2$ and $Mn_{0.7}Fe_{0.3}Si_2$ disc-shaped targets. The $MnSi_2$ and $Mn_{0.7}Fe_{0.3}Si_2$ targets were respectively irradiated by a pulsed laser with a wavelength of 266 nm to grow $MnSi_\gamma$ and $Mn_{0.7}Fe_{0.3}Si_\gamma$ thin films on an R-sapphire substrate. The substrate temperature was kept at 973 K during the growth. The film thicknesses of $MnSi_\gamma$ and $Mn_{0.7}Fe_{0.3}Si_\gamma$ thin films were 98 nm and 87 nm, respectively. In order to characterise the crystal structure of the thin films, X-ray diffraction (XRD) patterns were measured using a CuKα radiation source (D8 ADVANCE, BRUKER), and Raman spectroscopy using a laser source with a wavelength of 532 nm (NRS5100, JASCO) was performed. The band gap was investigated by ultraviolet-visible-NIR (UV-Vis-NIR) spectroscopy (UV-3600, Shimadzu). The XRD patterns, Raman spectra and UV-Vis-NIR spectra were obtained at room temperature. The Seebeck coefficient was evaluated by measuring an induced voltage in response to a temperature difference up to 0.5 K between the both ends of the film surface.

3. Results and discussion

Fig. 2 shows the electronic band structure along some high symmetry lines in the tetragonal Brillouin zone of (a) $Mn_{11}Si_{19}$ and (b) $(Mn_{31/44}Fe_{13/44})_{11}Si_{19}$, which are the model structures of $MnSi_\gamma$ and $(Mn_{0.7}Fe_{0.3})Si_\gamma$, respectively. The Fermi level, E_F, crossed some valence

Download English Version:

https://daneshyari.com/en/article/7832976

Download Persian Version:

https://daneshyari.com/article/7832976

Daneshyari.com